



The University of Bradford Institutional Repository

<http://bradscholars.brad.ac.uk>

This work is made available online in accordance with publisher policies. Please refer to the repository record for this item and our Policy Document available from the repository home page for further information.

To see the final version of this work please visit the publisher's website. Access to the published online version may require a subscription.

Link to publisher's version: <http://seekdl.org/visitor.php?id=4417>

Citation: Anoh KOO, Abd-Alhameed RA, Ochonogor O, Dama YAS, Jones SMR and Mapoka TT (2014) Performance evaluation of raised-cosine wavelet for multicarrier applications. *International Journal of Environmental Engineering*. 1(3): 1-5.

Copyright statement: © 2014 The IRED Scientific Publishing. Full-text reproduced in accordance with the publisher's self-archiving policy.

Performance Evaluation of Raised-Cosine Wavelet for Multicarrier Applications

KOO Anoh¹, RAA Abd-Alhameed¹, O Ochonogor², YAS Dama³, SMR Jones¹ and TT Mapoka¹

Abstract – Wavelets are alternative building kernels of the multicarrier systems, such as the orthogonal frequency division multiplexing (OFDM). The wavelets can be designed by changing the parent basis functions or constructing new filters. Some two new wavelets are considered for multicarrier design; one is designed using raised-cosine functions while the other was constructed using ideal filters. The spectrums of raised-cosine wavelet filters are controlled by a roll-off factor which leads to many distorting sidelobes. The second family of wavelet, which the raised-cosine wavelet is compared to, have no distorting sidelobes. It will be shown that raised-cosine wavelets are less suitable for multicarrier design in multicarrier environment, in terms of BER when compared to the wavelet constructed from the ideal filter.

Keywords–wavelet; raised-cosine; ideal filter; OFDM; multicarrier system;

I. INTRODUCTION

The wireless communications standards evolve with different new technologies. As an example, in the baseband of most recent wireless communications standards such as the LTE-Advanced (LTE-A), the orthogonal frequency division multiple access (OFDMA) is used [1] as the air-interface wireless protocol that can support multicarrier system (MCS) design to combat intersymbol interference (ISI). On the other hand, using wavelet transform (WT) to design MCS would reduce its sensitivity to ISI and intercarrier interference (ICI) [2, 3]. Additionally, WT can operate MCS without a cyclic prefix (CP) hence maximizing the spectral efficiency. These wavelets are orthonormal functions that can be designed either by changing the parent basis function or by constructing new filters [4]. Examples of these filters that can construct MCS are discussed in [5-9]. In closed-form expression, [8] provided two raised-cosine functions to design wavelets. As much as we know, no author has reported its application, for instance in the design of MCSs over frequency selective channel. Although traditional wavelets exist (see [10] and references therein), [8, 9, 11] have pursued the construction of additional wavelets using different filter approximations. Of particular

interest, these wavelets reported in [9] and [8] will be assessed in terms of BER performance over frequency selective channel with additive white Gaussian noise (AWGN) in this study. The wavelet in [11] was shown to be similar to the Daubechies wavelets in which the orthogonal wavelets reported in [9] were shown to outperform.

Wavelets are orthogonal functions and have found applications in many fields such as pharmacodynamics [12], channel modelling [13], etc. They operate using filter bank. For any filter chosen, appropriate cut-off frequency or proper approximation solution of the ideal filters must be carefully selected for excellent signal analyses and system performance. Some filters are preferred in one wavelet design over another. For example, the biorthogonal filters are preferred in image processing due to efficient image boarder resolution against the orthogonal filters [10]. On the other hand, orthogonal wavelets are preferred against biorthogonal wavelets in digital signal processing [10] because the orthogonal wavelets have better orthogonal basis to process, for instance, multicarrier signals. Since wavelets can be designed for different interests, [4] has outlined several algorithms for designing wavelets to match any signal of interest. In [9], these algorithms were exploited to design multicarrier communication systems by constructing entirely new filters for wavelet filter banks based on ideal filters. By constructing an appropriate low-pass filter (LPF) that suits band-limited conditions, the new wavelet in [9] was designed. Since the filters that constitute the filter banks in orthogonal wavelets design are complementary, the corresponding high-pass filter (HPF) can also be realized. The wavelet reported in [9] was shown to be better than the conventional wavelets in MCSs over multipath environment. In this study, we apply the raised-cosine wavelets in the design of MCSs and compare them with the ideal-filter based wavelets.

We will discuss the system model in Section II, the wavelet-based MCS in Section III and the simulation results in Section IV. The conclusion will be presented in Section V.

II. SYSTEM MODEL

The system model presented is a single input single output (SISO) wireless communication system using the wavelet transform as the baseband kernel. Its channel model is the wide-sense stationary uncorrelated scattering (WSSU) model discussed by Bello (see [14]) and widely used to model the multipath channel. The narrowband complex channel response is represented by the stochastically time-

¹Mobile and Satellite Communications Research Centre, University of Bradford, UK

²Dept. of Electronics Engineering, University of Westminster, UK

³An-Najah National University, Nablus, Palestine

varying

variable

$h = \alpha + j\beta = \sqrt{\alpha^2 + \beta^2} \cdot e^{-j\arctan(\beta/\alpha)} = |h| \cdot e^{j\theta}$, with $|h|$ as the fading envelope of the narrowband between the receiver and the transmitter. This model is a Rayleigh distribution if α and β are Gaussian distribution random variables with zero mean and i.i.d. In multipath transmission, α and β are typically complex variables that are uncorrelated [15] for individual path traversed. Meanwhile with OFDM, the channel selectivity is reduced to flat fading. Thus, the correlation difference among the paths traversed by the transmitted signal becomes quite infinitesimal. In a multipath-concerned design, a multicarrier system can be generally represented for a received signal of a SISO system as:

$$X = HS + Z \quad (1)$$

where $X \in C^{N \times 1}$ is the received signal, $diag\{H\} \in C^{N \times N}$ represents the channel, $S \in C^{N \times 1}$ is the transmitted signal and $Z \in C^{N \times 1}$ is the AWGN. Notice that H is the channel transfer function of the channel impulse response (h). Also, notice that the AWGN is characterized by $Z \sim \mathcal{N}(0, \sigma^2 I_{N \times N})$ and satisfies $Z[i] \neq Z[j]$ for all $i, j = 0, 1, \dots, N-1$. The term $C^{N \times N}$ represents a matrix with complex elements of dimension $N \times N$. σ is the standard deviation and σ^2 is the variance of Z . Again $\sigma^2 I_{N \times N}$ is an identity matrix of $N \times N$ dimension with σ^2 as the diagonal elements.

From Equation 1, the time domain equivalent of the transmitted signal can further be expressed as:

$$s(t) = \sum_{n=-\infty}^{+\infty} \sum_{m=0}^{N-1} a_{m,n}(t) \varphi_{m,n}(t) \quad (2)$$

where $a_{m,n}(n \in Z, m = 0, 1, \dots, N-1)$ represents the complex discrete Fourier transform (DFT) in the conventional OFDM. Each of such OFDM symbol will be conveyed by m^{th} subcarrier of the $\varphi_{m,n}(t)$ during n^{th} symbol time. Here, $\varphi_{m,n}(t)$ is the synthesis basis function which is obtained by time-frequency translation of the prototype filter function $\varphi(t)$ in DFT-OFDM. The total symbol time will be $T_{tot} = T_s + T_{cp}$ and has nT_{tot} sampling periods. Such prototype filter can be expressed as:

$$\varphi_{m,n}(t) = e^{j2\pi m f_{sc} t} \varphi(t - nT_{tot}) \quad (3)$$

where f_{sc} is the frequency spacing among the subcarriers. In the conventional OFDM, $\varphi(t)$ is rectangular function defined as [16]:

$$\varphi(t) = \begin{cases} \frac{1}{\sqrt{T_{tot}}}, & -T_{cp} \leq t \leq T \\ 0, & \text{otherwise} \end{cases} \quad (4)$$

Substituting Equation 4 into 3, and then substituting the result into Equation 1, it is obtained that:

$$s(t) = \frac{1}{\sqrt{T_{tot}}} \sum_{m=0}^{N-1} a_{m,n} e^{j2\pi m f_{sc} t} \quad (5)$$

Here, Equation 4 represents the analytical expression of the conventional CP-based OFDM. $\varphi(t)$ can assume other forms of filter functions for different multicarrier system kernels. A handy example is the wavelet transform scaling function.

Wavelet multicarrier systems are filter bank based MCSs and so, can operate without the CP. Since filter bank MCSs operate without a CP [16], we proceed to discussing signal transformation that precludes any CP.

III. WAVELET-OFDM

The wavelet OFDM is obtained by substituting the WT filters for DFT filters in the conventional OFDM design architecture. Two different WT construction functions are discussed; each is discussed in Subsections II-B and III-C. The basic wavelet theory is reviewed first in Section III-A.

A. Basic wavelet theory

Given that $a_{m,n}(t)$ modulates the transforming function $\varphi(t)$. The $\varphi(t)$ is a scaling function and also represents the prototype filter basis function as in Equation 5. In discrete form, the input signal can be combined with $\varphi(t)$ as [17];

$$S_{DWT} = \sum_{n=0}^{N-1} \sum_{m=0}^{M-1} a_{m,n}(t) \varphi_{m,n}(t) \quad (6)$$

where M is the length of the characteristic filter. The scaling function is weighted at each time-shift (m) as:

$$\varphi(t) = \sqrt{2} \sum_m b(m) \varphi(2t - m) \quad (7)$$

where $b(m)$ is the weight or LPF. The LPF is complementary to the high-pass filter (HPF) in filter banks of orthogonal wavelets. The former constructs the approximate coefficient part of the signal while the later constructs the detail coefficient part of the signal. Both LPF and HPF are related as [9]:

$$b(m) = (-1)^m g(M-1-m) \quad (8)$$

$g(m)$ is the HPF.

B. Construction of wavelets using the root-raised function

There are two scaling functions constructed from root-raised cosine function to describe wavelet transforms. The first example of these functions was derived differently but with similar results by [18] and [8] as:

$$\varphi_1(t) = \frac{\sin \pi(1-\beta)t + 4\beta t \cos \pi(1+\beta)t}{\pi(1-(4\beta t)^2)} \quad (9)$$

Later, [19] classified φ_1 as a member of the Meyer functions provided $\beta=1/3$. A second class of this wavelet function was only defined by [8] as:

$$\varphi_2(t) = \frac{\sin \pi(1-\beta)t + \sin \pi(1+\beta)t}{2\pi(1-2\beta t)} \quad (10)$$

where β is the roll-off factor of the raised-cosine function. The roll-off factor influences the filter properties of these wavelets. For instance, the side-lobes of the root-raised filter are controlled by the prevailing roll-off factor (see Figure 1).

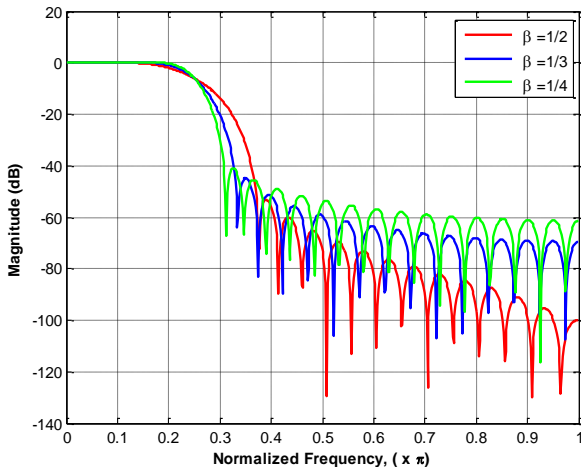


Figure 1: Side-lobes of root-raised cosine filter function

From Figure 1, the side-lobes of the roll-factor $\beta = 1/2$ are mostly suppressed amongst all, although least spectrally efficient. In that case, the $\beta = 1/3$ is more efficient than $1/2$ but less efficient than $1/4$. Meanwhile, the side-lobes of the $\beta = 1/2$ are most well suppressed followed by those of $1/3$. In all cases, $1/3$ is most likely in trade-off in terms of efficiency and well-suppressed side-lobes compared to $1/2$ and $1/4$. In [8, 19], $\beta = 1/3$ was preferred. Thus, $\beta = 1/3$ will be used throughout in this study. However, it can be inferred that the roll-off factor influences the behaviour of any raised cosine-function filter and would influence the performance of the dependent wavelet.

C. Wavelet Construction from ideal filters

Define an ideal filter of order 4, [9] showed that;

$$B(\omega) = b(0) + b(1)e^{-j\omega} + b(2)e^{-j2\omega} + b(3)e^{-j3\omega} \quad (11)$$

where $B(\cdot)$ is the filter response. From the symmetry condition shown in [9],

$$b(0) = b(3)$$

and

$$b(1) = b(2)$$

Finally, the resulting filter coefficients are defined as:

$$b(0) = 1/4 \left(1 - \frac{\sqrt{2}}{2} \right) \quad (12)$$

$$b(1) = 1/4 \left(1 + \frac{\sqrt{2}}{2} \right)$$

This is the low-pass filter required to build the MCS. The filter is distortionless and so free from ISI [9] as shown in Figure 2 and also will be less influenced by ICI like in [2, 3]. On the other hand, the raised-cosine filters depend on the roll-off factor. In any selected wide-bandwidth and with DFT filters for instance, the DFT splits the spectrum into as many DFT points as required to create narrowbands. These narrowband subcarriers can be bandlimited by windowing,

else, using the roll-off factor is significantly the only way to bandlimit the subcarriers. Meanwhile, the noise power in a system is a function of the spectrum/bandwidth of transmission. Then by reducing the bandwidth, the noise power in the system can be reduced. But, reducing the bandwidth too much distorts the pulse-shape and introduces longer “ringing” of the sidelobes, and in turn introduces intersymbol interference. This will thus impair the raised-cosine wavelet in BER performance as will be seen shortly in the results.

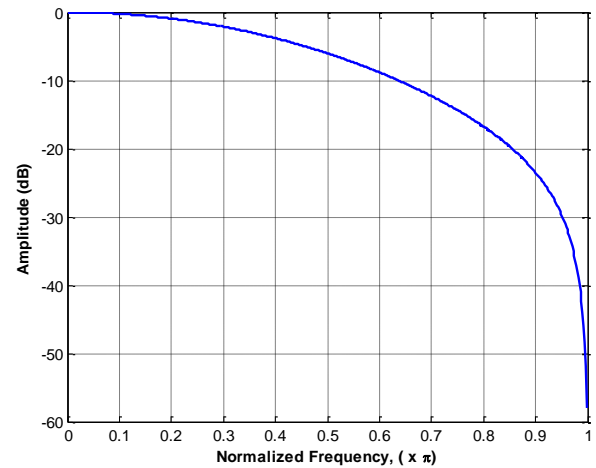


Figure 2: Ideal-filter showing no side-lobes

These limitations found in raised-cosine functions, e.g. the sidelobes shown in Figure 1 are absent in the case of the ideal-filter based wavelets of [9] which have no sidelobes as shown in Figure 2.

IV. SIMULATION RESULTS AND DISCUSSION

Figure 3 shows a high-level representation of the multicarrier modulation transceiver using the WT over multipath environment.

A. System Implementation

The input signal are randomly generated and mapped using the BPSK mapping scheme. Then using inverse-WT (IWT), the signal is transformed and the resulting signal transformed into frequency domain which is convolved with the channel transfer function of the multipath channel model.

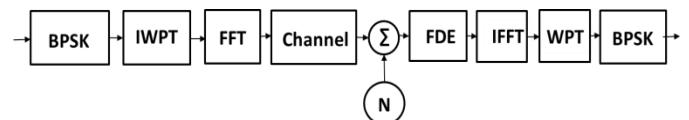


Figure 3: Multicarrier modulation using wavelet transform over multipath channel

This is passed through AWGN noise then received in the receiver. By some channel compensation as described in Section IV-B the signal is received and transformed back into the wavelet-domain using the FFT for onward WT demodulation. The received signals are demapped using BPSK before performing error estimation. In the second

case, the process is repeated but BPSK is replaced with QPSK.

B. Equalization

In [9], some frequency domain equalization (FDE) was described. It involved transforming the frequency content of $s(t)$, as a Fourier transform pair; $S(f) \leftrightarrow s(t)$, where FT is the Fourier transform. From Equation 1, the convolution of the signal and the channel transfer function is defined from;

$$X(f) = H(f) \otimes S(f) + Z(f) \quad (13)$$

This is the frequency domain equivalent of the received signal with $Z(f)$ as the AWGN. In the receiver, the equalization follows as:

$$\hat{X} = \frac{H^H \times X}{\|H\|^2} = \frac{H^H \times H \otimes S}{\|H\|^2} + \frac{H^H \times Z}{\|H\|^2} \quad (14)$$

where $(\cdot)^H$ is a Hermitian operator, \otimes and $(\cdot)^*$ are convolution and conjugation operators respectively. Also $\|\cdot\|$ describes absolute operator. Suppose that the channel response could be negligible, such that $|H| \rightarrow 0$, then some error correction parameter, ε , will be introduced as follows:

$$\hat{X} = \frac{H^H \times X}{\|H\|^2 + \varepsilon} = \frac{H^H \times H \otimes S}{\|H\|^2 + \varepsilon} + \frac{H^H \times Z}{\|H\|^2 + \varepsilon}, \quad 0 \leq \varepsilon \leq 1 \quad (15)$$

Notice that \hat{X} is the frequency domain content of the received signal after the FDE equalization. Now, using the inverse FFT (IFFT) the received signal is transformed into the wavelet domain before demodulating by the forward WT.

C. Results and Discussion

As described in Section IV-A, the system was modelled for a BPSK mapping scheme, in one case, with 64 symbol length averaged over 37000 symbols. Secondly, the design is then modified to include the QPSK mapping scheme with similar design environments using similar parameters. No form of coding has been applied.

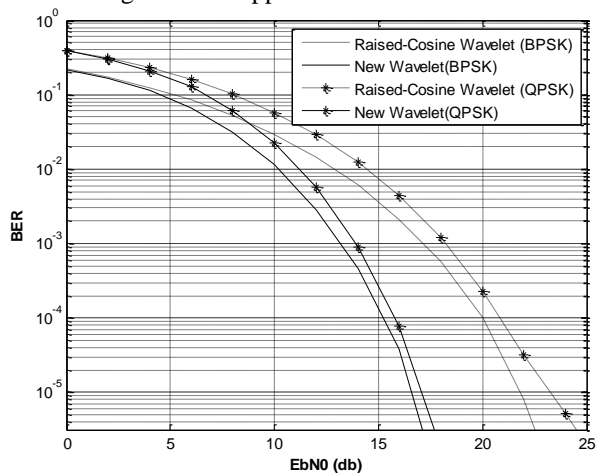


Figure 4: Comparison of ideal-filter wavelet with Root Raised Cosine Wavelet ($\beta=1/3$) over multipath channel with AWGN for φ_1 .

Meanwhile, Figures 4 and 5 show our results for BPSK and QPSK for the two families of wavelets discussed in Sections III-B and III-C. For compactly supported wavelets, using lower order filter lengths will reduce the simulation runtime, and of course the associated overheads (see Ch. 13 of [20]). We show in Figure 4 the results of BER performances of raised-cosine wavelets with ideal-filter based wavelet. Both are operated as orthogonal wavelets. The roll-off factor maximizes the spectrum of its pulse and also the raised-cosine wavelets. In band-limited signal processing, the frequency spectrum of every subcarrier signal in OFDM is not a band-limited sampling function, and so every subcarrier will produce side-lobes in the frequency domain resulting from the truncation of a rectangular or another type of window [2]. For the raised-cosine filter, the spectrum is predetermined by the roll-off factor. Although the noise power would be reduced by the 1/3 roll-off factor, the distortion produced in the pulse by the roll-off factor depletes the BER performance against the distortionless ideal-filter wavelet.

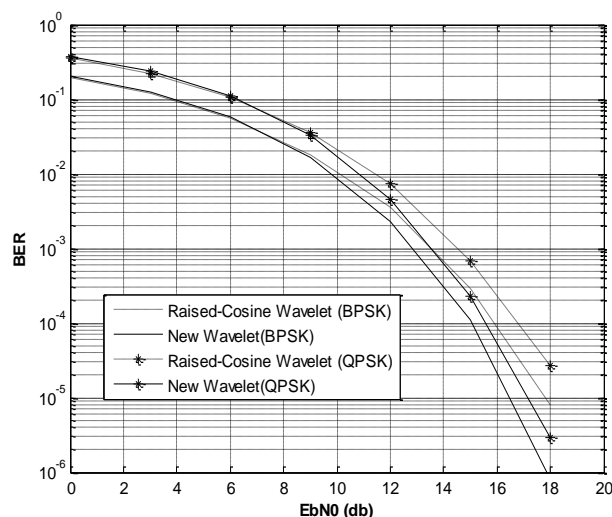


Figure 5: Comparison of ideal-filter wavelet with Root Raised Cosine Wavelet ($\beta=1/3$) over multipath channel with AWGN for φ_2 .

Our results show that the raised-cosine wavelets are performing less than the ideal-filter orthogonal wavelets that has maximally flat sidelobes; this accounts for the circa 1db better performance than the raised-cosine wavelet. This phenomenon is again reflected in Figure 5 for φ_2 .

The roll-off factor determines the behaviour of a raised cosine filter in terms of the bandwidth and sidelobes. It also influences the length of “ringing” of the sidelobes of the filter. The length of the sildelobes will affect also the peak-to-average power ratio (PAPR) due to out-of-band emissions from the *ringings* that may increase the energy in the adjacent subcarrier mainlobes. Against the trade-off in the raised-cosine filter design provided by the 1/3 roll-off factor, our results show that the raised-cosine wavelet can be less preferred to the orthogonal wavelets reported in this work in terms of BER.

V. CONCLUSION

Alternative multicarrier building kernels have been presented. They are the wavelet MCSs. One family of the wavelets considered was designed from the raised-cosine filter function while the other was constructed from the ideal filter. Both were compared over a WSSU multipath environment. These comparisons were based on their respective performances using the BER statistics curves. It was found that the performances of the raised-cosine filter-based wavelets are less than the ideal filter wavelets in terms of BER statistics measures. It follows that, in designing MCSs, the raised-cosine wavelets cannot be preferred over the rest orthogonal wavelets. It may however find suitable application in other areas, may be in terms of biorthogonal wavelets; but it cannot be recommended for MCSs design.

REFERENCES

- [1] Y.-H. Nam, L. Liu, Y. Wang, C. Zhang, J. Cho, and J.-K. Han, "Cooperative communication technologies for LTE-advanced," in *2010 IEEE International Conference on Acoustics Speech and Signal Processing (ICASSP)*, 2010, pp. 5610-5613.
- [2] Y. Zhang and S. Cheng, "A novel multicarrier signal transmission system over multipath channel of low-voltage power line," *IEEE Transactions on Power Delivery*, vol. 19, pp. 1668-1672, 2004.
- [3] B. Negash and H. Nikookar, "Wavelet based OFDM for wireless channels," in *IEEE VTS 53rd Vehicular Technology Conference, 2001. VTC 2001 Spring*, 2001, pp. 688-691.
- [4] J. O. Chapa and R. M. Rao, "Algorithms for designing wavelets to match a specified signal," *IEEE Transactions on Signal Processing*, vol. 48, pp. 3395-3406, 2000.
- [5] M. G. Bellanger, "Specification and design of a prototype filter for filter bank based multicarrier transmission," in *2001 IEEE International Conference on Acoustics, Speech, and Signal Processing, 2001. Proceedings (ICASSP'01)*, 2001, pp. 2417-2420.
- [6] A. Viholainen, T. Ihalainen, T. H. Stitz, M. Renfors, and M. Bellanger, "Prototype filter design for filter bank based multicarrier transmission," in *Proceedings of European Signal Processing Conference (EUSIPCO)*, 2009, p. 93.
- [7] A. Şahin, I. Güvenç, and H. Arslan, "A Survey on Prototype Filter Design for Filter Bank Based Multicarrier Communications," *arXiv preprint arXiv:1212.3374*, 2012.
- [8] G. Walter and J. Zhang, "Orthonormal wavelets with simple closed-form expressions," *IEEE Transactions on Signal Processing*, vol. 46, pp. 2248-2251, 1998.
- [9] K. O. O. Anoh, J. M. Noras, R. A. Abd-Alhameed, S. M. R. Jones, and K. N. Voudouris, "A New Approach for Designing Orthogonal Wavelets for Multicarrier Applications," *AEU - International Journal of Electronics and Communications*, 2014.
- [10] O. O. Anoh, R. A. Abd-Alhameed, S. M. R. Jones, Y. A. S. Dama, J. M. Noras, A. M. Altimimi, N. T. Ali, and M. S. Alkhambashi, "Comparison of Orthogonal and Biorthogonal Wavelets for Multicarrier Systems," *International Design and Test Symposium*, Dec. 15 - 17, 2012 2012.
- [11] R. Ansari, C. Guillemot, and J. Kaiser, "Wavelet construction using lagrange halfband filters," *IEEE Transactions on Circuits and Systems*, vol. 38, pp. 1116-1118, 1991.
- [12] D. E. Mager and D. R. Abernethy, "Use of wavelet and fast Fourier transforms in pharmacodynamics," *Journal of Pharmacology and Experimental Therapeutics*, vol. 321, pp. 423-430, 2007.
- [13] O. A. Aboaba and K.-S. Chung, "Multipath Channel Parameter Estimation in Mobile Radio Environments Using Stationary Wavelet Transform," in *2005 Asia-Pacific Conference on Communications*, 2005, pp. 203-207.
- [14] M. Pätzold, A. Szczepanski, and N. Youssef, "Methods for modelling of specified and measured multipath power delay profiles," *IEEE TRANSACTION ON VEHICULAR TECHNOLOGY* vol. 51, pp. 978 - 988, 2002.
- [15] M. K. Simon and M.-S. Alouini, *Digital communication over fading channels* vol. 95: Wiley-Interscience, 2005.
- [16] J. Du and S. Signell, "Comparison of CP-OFDM and OFDM/OQAM in doubly dispersive channels," in *Future Generation Communication and Networking (FGCN 2007)*, 2007, pp. 207-211.
- [17] K. O. O. Anoh, R. A. Abd-alhameed, J. M. Noras, and S. M. R. Jones, "Wavelet Packet Transform Modulation for Multiple Input Multiple Output Applications," *IJCA*, vol. 63 - Number 7, pp. 46 - 51, 2013.
- [18] S. Chennakeshu and G. Saulnier, "Differential detection of $\pi/4$ -shifted-DQPSK for digital cellular radio," *IEEE Transactions on Vehicular Technology*, vol. 42, pp. 46-57, 1993.
- [19] W. W. Jones and J. C. Dill, "The square root raised cosine wavelet and its relation to the Meyer functions," *IEEE Transactions on Signal Processing*, vol. 49, pp. 248-251, 2001.
- [20] I. Glover and P. M. Grant, *Digital communications*: Pearson Education, 2010.